Photodegradation of Norfloxacin on $Ni_{0.5}Cd_{0.5}S/g\text{-}C_3N_4$ Composites in Water

Qinjun Chen, Guoqiang Lai, Zanen Wu, Xia Chen*, Jinhui Zhang, Shibiao Wu**
Anhui Province Key Laboratory of Advanced Building Materials, Anhui Jianzhu University, Ziyun Road, 230601, Hefei, Anhui, China.
chenxhl@ahjzu.edu.cn*, wsbl@ahjzu.edu.cn**

(Received on 29th February 2024, accepted in revised form 13th November 2024)

Summary: Widely used in hospital and animal farming, the large amounts of norfloxacin (NORF) were discharged into the water environment which caused severe pollution problems. Photocatalysis technology can decompose, mineralize most organic compounds, including NORF. In this paper, $Ni_{0.5}Cd_{0.5}S$(NCS), g-C_3N_4(CN) and their composites were prepared as photocatalysts. The composites were characterized by SEM, energy-disperse X-ray spectroscopy (EDS) and XRD. It was showed that NORF in water can be effectively removed by NCS/CN composites in visible light. The experimental results proved that the composites have better photocatalytic degradation performance than NCS or CN alone. The best photocatalysis reaction condition of pH was 7. There were different performances on the degradation of NORF when the interfere anions, NO_3^-, C^- and HCO_3^-were mixed in the reactive system. $HCO_3^-$and Cl^- were the inhibitory substances on the photocatalysis reaction, and NO_3^- slightly prompted the reaction. In addition, the main active substances produced in the reaction were superoxide radicals ($\bullet O_2^-$) and holes (h^+) which were confirmed by adding different free radical quenchants in NORF photodegradation reaction system.

Key words: $Ni_{0.5}Cd_{0.5}S$; g-C_3N_4; Composites; Norfloxacin; Photocatalysis.

Introduction

NORF is one of the most widely used antibiotics in medical industry and animal farming. With the mass production and consumption, the large amounts of NORF were discharged into the water environment which caused severe pollution problems[1]. Only a small fraction of NORF could be digested by humans or animals, about 90 percent were released into the environment. In many agricultural areas, antibiotics were applied to farmland irrigation with wastewater and penetrate into the surrounding environment through leaching, which makes antibiotics accumulate continuously in the environment and cause harm to the surrounding environment[2]. The accumulated antibiotics could cause antibiotic resistance genes (ARG) and the proliferation of drug-resistant bacteria (ARB), which seriously affects the balance of ecosystems. There are many treatments technology to remove NORF from wastes water, including biological sewage treatment[3], adsorption method[4], advanced oxidation process[5] and photocatalytic degradation[6],etc. NORF is difficult to be efficiently degraded by conventional biological sewage treatment method because the biochemical resistance of NORF. The disadvantage of adsorption is that the processing capacity is small and advanced oxidation technology would consume a lot of chemicals. Photocatalytic degradation is an energy-saving and environmentally friendly processes and can decompose, mineralize most organic compounds, including NORF.

There are many kinds of photocatalyst materials, among which CdS is a remarkable photocatalytic material with a band gap of 2.43eV[7], which is far greater than 1.8eV, the average photon energy in solar spectral[8, 9]. In order to reduce the bandgap of the material, CdS doping with nickel [10](NCS) would be a promising strategy to reduce the bandgap of the photocatalyst.

g-C_3N_4 (CN) is another promising photocatalyst with a bandgap of 2.7eV[11] and the material cannot be excited by the main visible light energy in the solar spectrum; in order to extended light response wavelength range of CN, the composition of NCS and CN is a favorable method . In addition, the composite material can also improve the photogenerated electrons and holes recombination of NC in the photocatalytic process[12].

*To whom all correspondence should be addressed.

In this paper NCS/CN composites were synthesized by hydrothermal method. The morphology and structure of the composites were characterized. The NORF photodegradation performances of the composites in water were studied. The experimental results proved that the composites have better photocatalytic degradation performance than NCS or CN alone. The best photocatalysis reaction condition of pH was neutral. There was different performance on the degradation of NORF when the interfere ions were mixed in the reactive system. HCO_3^- ion was the inhibitory substance on the photocatalysis reaction, an NO^-, Cl^- slightly prompted the reaction. In addition, the main active substances produced in the reaction were confirmed by adding different free radical quenchants in NORF photodegradation reaction system.

Experiments

Materials

Urea was purchased from Shanghai SuYi Chemical Reagent Co., Ltd. Cadmium acetate ($Cd(Ac)_2·2H_2O$) and Nickel acetate tetrahydrate ($Ni(Ac)_2·4H_2O$) were obtained from Shanghai Aladdin Biochemical Technology Co., Ltd. Thioacetamide was purchased from Macklin. Sulfuric acid(H_2SO_4,98%), sodium bicarbonate ($NaHCO_3$), sodium hydroxide (NaOH), sodium chloride (NaCl), sodium nitrate ($NaNO_3$) and ethylene diamine tetraacetic acid (EDTA) were from Sinopharm Group Chemical Reagent Co., LTD. Ethanol, isopropanol (IPA) and p-benzoquinone (BQ) were purchased from Aladdin. Norfloxacin（NORF） was from Adamas Reagent Co., LTD. All reagents were analytically pure and used directly without further purification. Ultrapure water(18MΩ) was prepared by an Aquapro machine(AWL-10001-M).

Preparation of CN

Preparation of carbon nitride coarse powder

First, we weighed 5 g of urea into the porcelain boat and capped it. Secondly, the porcelain boat was placed in the Muffle furnace with the heating rate set at 2 ℃/min. After heating to 500 ℃ and constant temperature for 120 min, the light yellow carbon nitride coarse powder (bg-C_3N_4) was obtained after natural cooling to room temperature.

Preparation of Nanosheet CN

0.5g prepared block bg-C_3N_4 was added into 15 mL concentrated sulfuric acid, stirred magnetically for 72 h at room temperature until completely peeled off, and then the mixed solution and ethanol were added into ethanol according to the volume ratio of 1:3, and the product was continuously separated under continuous agitation. Secondly, the precipitation is separated by centrifugation, and the excess chemical residue is removed by centrifugal washing with deionized water several times, until the pH value of the solution is close to neutral, and the obtained sample is freeze-dried in the freeze-drying machine. Finally, CN nanosheets with good dispersion can be obtained by drying them in an oven at 50°C for 2 h.

Preparation of NCS/CN

10 mL 4 M NaOH solution was poured into 60 mL water solution containing 2.142g (0.00804mol) $Cd(Ac)_2·2H_2O$ and 2.00g(0.00804mol) $Ni(Ac)_2·4H_2O$. 1.761g(0.0234mol) thioacetamide and 0.5g CN were added into the above solution, uniformly dispersed by ultrasonic and stirred continuously for 20 minutes. The mixture was packaged in a 100 mL reactor in a drying oven at 180℃ for 24 h. After natural cooling, the solid-liquid mixture was centrifuged and the crude product was black solid. After washing with ethanol for several times, NCS/CN composites was finally obtained, which were labeled NCS-CN-4. The preparation processes of NCS, CdS and other NCS/CN composites labeled NCS-CN-1,2,3 were similar to the procedure above, which making formulas were listed in Table-1.

Table-1: Formulas of materials.

Composite	CN(g)	$Ni(Ac)_2·4H_2O$ (g)	$Cd(Ac)_2·2H_2O$ (g)	thioacetamide (g)
NCS-CN-1	0.5	0.400	0.428	0.352
NCS-CN-2	0.5	0.800	0.857	0.704
NCS-CN-3	0.5	1.600	1.714	1.408
NCS-CN-4	0.5	2.000	2.142	1.761
NCS	0	2.000	2.142	1.761
CdS	0	0	4.284	1.761

Characterization

The morphology, composition and crystallinity of the catalyst were characterized by Hitachi Regulus 8100 electron microscope (SEM) and Rigaku Smartlab X-ray diffraction analyzer (XRD). The optical absorption properties of NORF solution were studied by UV-5500PC UV-VIS spectrometer. The maximum absorption wavelength was 278 nm.

Experimental

NORF was used as an organic pollutant to simulate the photocatalytic degradation experiment under the condition of sunlight irradiation, and 500 W xenon lamp with 420 nm filter was used as the light source. The degradation effect of NORF was evaluated by ultraviolet-visible spectrophotometer, which measured the change of the initial and final concentration of catalyst under the condition of light. The specific process was as follows:30 mg photocatalyst were mixed with 100 mL NORF solution (initial concentration=10mg/L, m/V=0.3g/L) in a 200mL beaker and stirred magnetically at 300 rpm for 60 min in dark to establish the adsorption-desorption balance. And then, a 300W xenon lamp was opened to irradiate on the top of the beaker for 120 minutes. During photodegradation, the reaction mixture was sampled by syringes at schemed time, and the samples were filtered by syringe filters (0.22 μm). The concentration of NORF was analyzed by an ultraviolet and visible spectrophotometer (UV-2550, Shimadzu, Japan) at 272nm. In the pH experiments, the pH values of solution were adjusted with a Rex pH meter (PHB-4, Shanghai, China) by adding 0.1 mol/L NaOH or H_2SO_4. In anions interference experiments, 0.001mol /L NaCl, $NaNO_3$ and $NaHCO_3$, as sources of Cl^-, NO_3^-an HCO_3^-, were added in reactor at the beginning of the experiments. In addition, 1.0mol /L EDTA, BQ and IPA as scavengers of h^+, $\cdot O^{2-}$ and ·OH were added in the photoreaction system when the free radicals trapping experiments were carried out. Unless mentioned, all initial pH of the NORF solution was 7.0. The temperature of the photodegradation experiments were all at 298K.

Results and Discussion

Structure and morphology of photocatalysts

In order to analyze the morphology characteristics of the catalyst, the surface of the material was scanned by electron beam of emission scanning electron microscope (SEM) to obtain the microstructure of the sample. Fig.1 (a) and (b) are the SEM of bulk carbon nitride and CN nanosheets respectively, which are analyzed in detail in the next chapter. Fig.1 (c) and (d) are the SEM of NCS and CdS, respectively. It can be clearly seen from Fig.1 (c), (d) NCS and CdS nanoparticles with uniform shape and tight arrangement. Because of the structure and morphology of NCS-CN-1,2,3,4 was similar, NCS-CN-3 was showed in Fig.1 as a representative. Fig.1(e) is the SEM mapping diagram of NCS-CN-3, and it can be clearly found from Fig.1(e) NCS nanoparticles are evenly and tightly wrapped on the surface of g-C_3N_4 nanosheets. Fig.1(f-j) represents EDS diagram of C, N, S, Ni and Cd elements respectively. It can be seen from observation that S, Ni and Cd elements are mainly distributed in the CNS nanoparticle region, while C and N elements are distributed in the surface of g-C_3N_4 particles. By observing the EDS map sum spectrum diagram of the composite and the inlet table in Fig.1(k), it can be seen that the atomic ratio of Ni and Cd elements is close to 1:1, which is consistent with the ratio of Ni and Cd sources in the preparation formulas, further proving that the successful preparation of NCS/CN composite.

Fig.2 shows the XRD patterns of different samples. The XRD pattern of massive carbon nitride shows that the positions of the two typical peaks of bg-C_3N_4 are 12.78˚ and 27.38˚ respectively, corresponding to the (001) and (002) crystal faces (JCPDS NO.87-1526). The two diffraction peaks at 12.78˚ and 27.38˚ correspond to the tritriazine ring plane repetition period and the layered structure periodic stacking of bg-C_3N_4, respectively. The XRD pattern of CN nanosheets obtained by sulfuric acid stripping showed two main characteristic peaks at 12.07˚ and 26.86˚, which were slightly shifted to a small angle compared with the massive carbon nitride. At the same time, it can be clearly seen that the diffraction peak intensity at 12.07˚ is very small or even negligible, which is caused by the increase in plane size and the decrease in structural defects of CN nanosheets after stripping with concentrated sulfuric acid compared with the massive carbon nitride.

The XRD pattern of NCS shows that the major diffraction peaks are 24.8˚, 26.5˚, 28.1˚, 36.6 ˚, 43.6 ˚, 47.8 ˚, and 57 ˚ which correspond to its (100), (002), (101), (102), (110), (103) and (201) crystal faces (JCPDS NO.41-1049), respectively. The XRD pattern of the NCS-CN-3 composite shows that the diffraction peak at 12.78˚ is from CN, the diffraction peaks at 24.8˚, 28.1˚, 43.6 ˚, 47.8 ˚ and 57˚ are from NCS, and the diffraction peak at 26.5˚ is from the superposition of the two. The analysis of XRD patterns above indicates the successful preparation of NCS/CN composites.

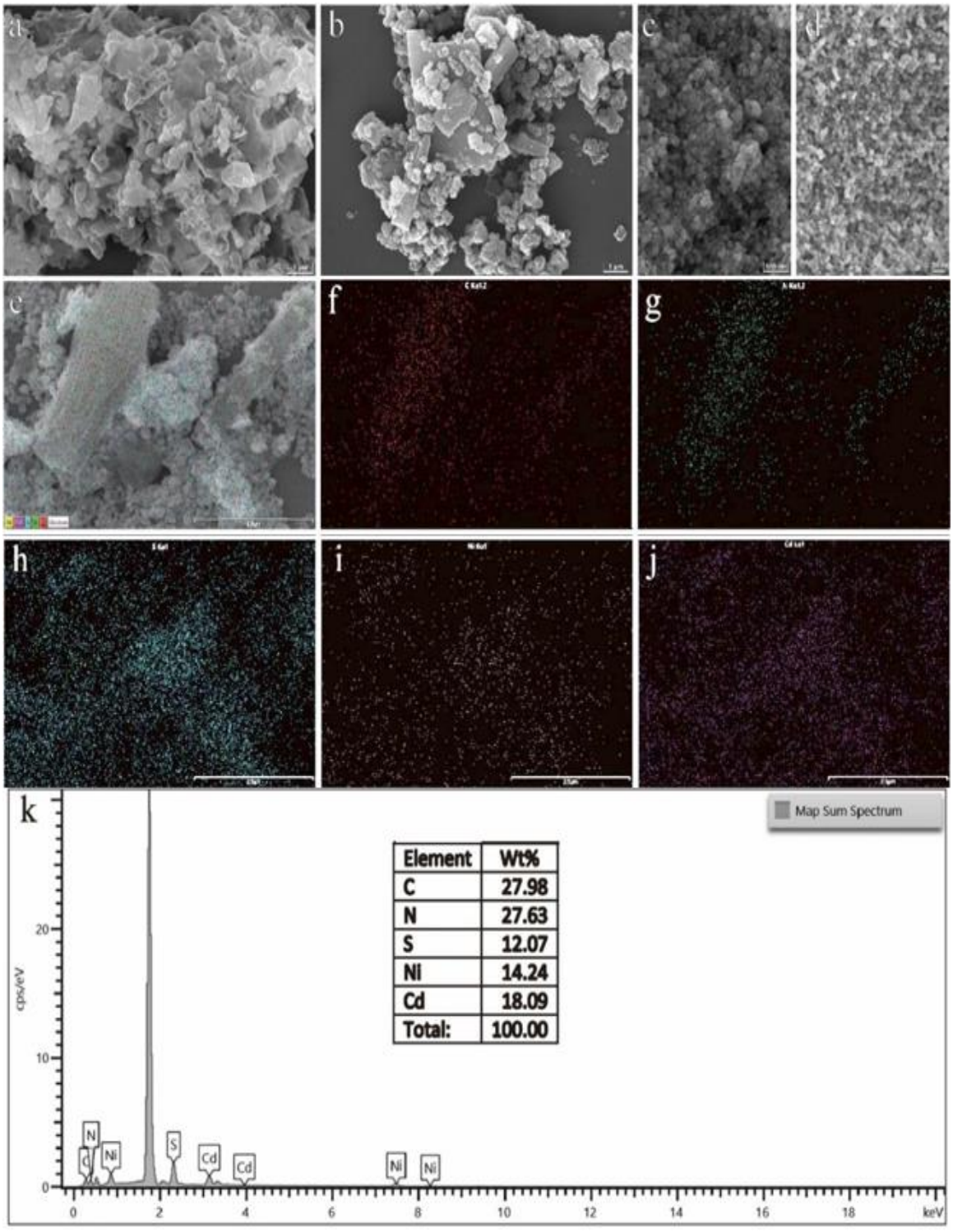

Fig. 1: (a-d) SEM of bg-C_3N_4, CN, NCS, CdS; (e) mapping diagram of NCS-CN-3; (f-j) distribution maps of elements C, N, S, Cd and Ni, respectively; (k) is EDS map sum spectrum of NCS-CN-3.

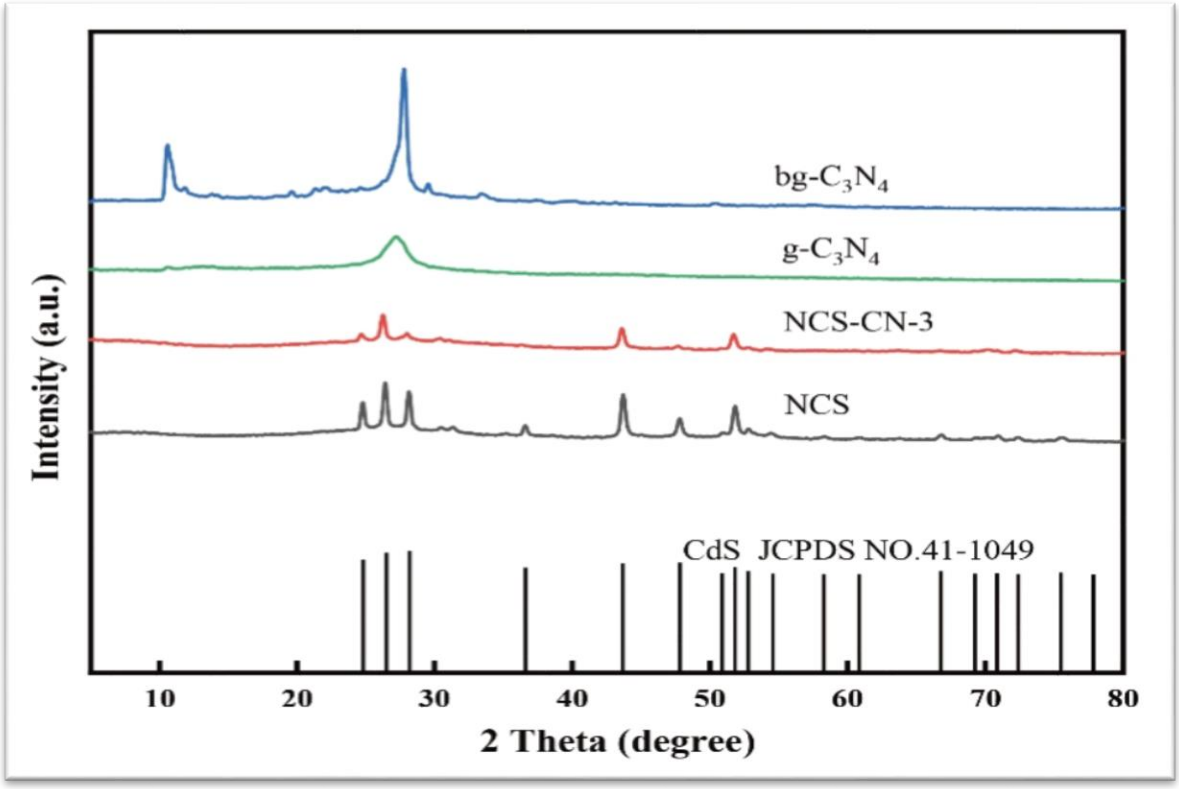

Fig. 2: XRD patterns of bg-C_3N_4, CN, NCS and NCS-CN-3 composites.

The light absorption characteristics of the photocatalyst were analyzed by UV-VIS diffuse reflectance spectroscopy. As shown in Fig.3 (a), the edge value of the light absorption band of NCS and NCS-CN-3 were at about 551 nm to 558 nm, and the CdS was at 470-500nm.

The band gap of semiconductor catalyst materials can be calculated by Tauc plot[13], described by equation (1):

$$(\alpha h\upsilon)^{\frac{1}{n}} = C(h\upsilon - Eg) \qquad (1)$$

where α is the absorption coefficient, h is Planck's constant, υ is the incident light frequency, C is a constant, Eg is the width of the band gap to be measured, where 1/n is 2 or 1/2 when the material is a direct band gap or an indirect band gap. Because CdS, NCS and CN were all the materials of direct band gap, 1/n is 2 here. Fig.3(b) showed the plot of $(\alpha h\upsilon)^2$ versus $h\upsilon$.When the linear portion of the curve is extended until it intersects with the X-axis, and the horizontal coordinate value at this intersection point corresponds to the bandgap of the material. As illustrated in Figure 3(b), the bandgaps of the synthesized NCS-CN-3, NCS, and CdS are 2.31 eV, 2.29 eV, and 2.48 eV, respectively. The incorporation of nickel atoms into the NCS results in a significant redshift in the absorption edge of the NCS photocatalyst, leading to a broader absorption edge. The bandgap of NCS is narrower than that of CdS, decreasing from 2.48 eV to 2.29 eV. In general, the bandgap of g-C_3N_4 is approximately 2.7 eV. However, the introduction of NCS reduces the bandgap of the synthesized NCS-CN-3 to only 2.31 eV, which is more suitable for harvesting solar energy within the visible spectrum. Given that the solar spectrum is predominantly composed of visible light, this narrow bandgap allows for a more effective utilization of solar energy, thereby enhancing the photocatalytic performance of NCS-CN-3.

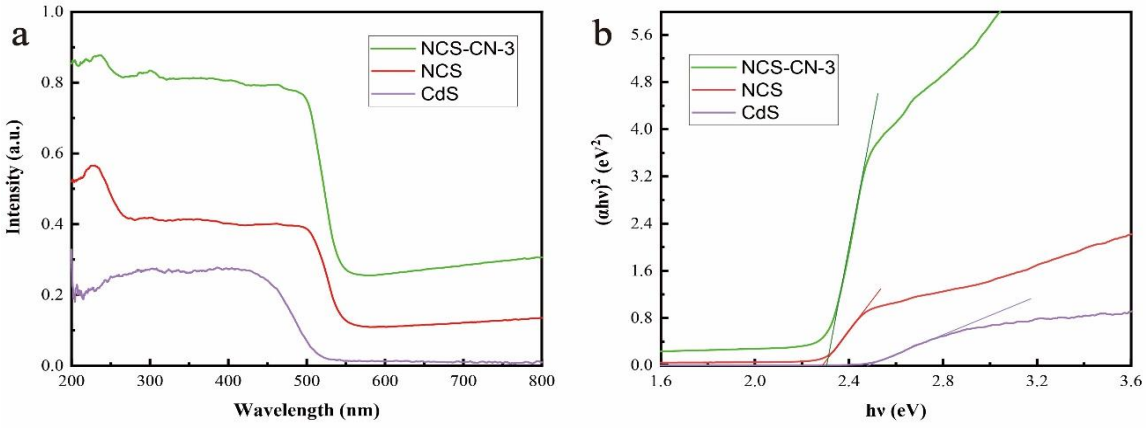

Fig.3 (a) UV-VIS absorption spectra and (b) bandgap energy of NCS-CN-3, NCS and CdS

Study on degradation of NORF

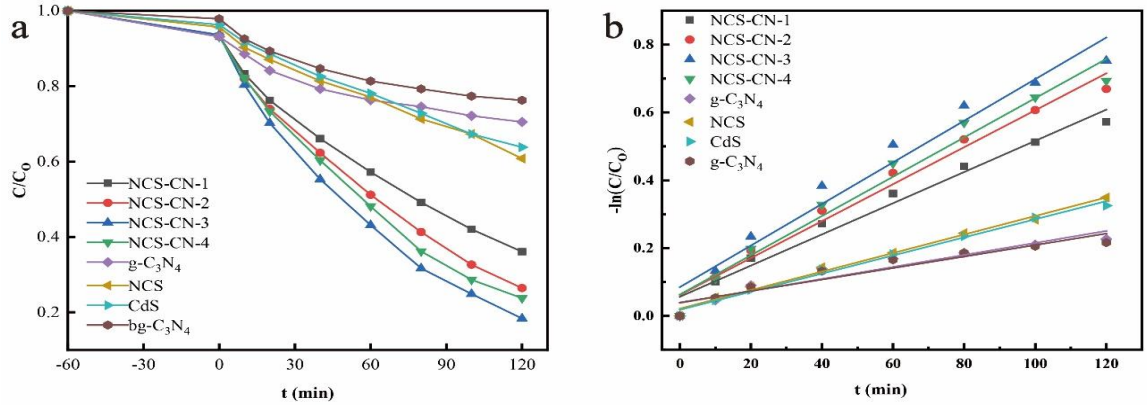

Fig.4:(a) photodegradation of norfloxacin on different materials. (b) different materials on the degradation rate of norfloxacin. m/V=0.3g/L, initial pH=7, $[NORF]_{initial}$=10mg/L, 298K.

Table-2: Slope and coefficient of determination for linear fitting of first-order dynamics.

Catalysts	$k_1(min^{-1})$	R^2
NSC-CN-1	**0.0046**	**0.9756**
NSC-CN-2	**0.0055**	**0.9778**
NSC-CN-3	**0.0061**	**0.9612**
NSC-CN-4	**0.0058**	**0.9715**
CN	**0.0018**	**0.9138**
NCS	**0.0027**	**0.9914**
CdS	**0.0026**	**0.9923**
bg-C_3N_4	**0.0017**	**0.9107**

The adsorption processes of NORF antibiotics on all materials in water under dark conditions were taken place before photocatalytic degradation. As can be seen from Fig.4(a), the NORF removal rates of different materials by dark adsorption were very close. However, in the control group experiments of photocatalytic degradation of NORF, the photocatalytic activity of single component catalysts, including bg-C_3N_4, CN, CdS and NCS, were obvious inferior to the photocatalysts of NSC-CN-1,2,3,4 composites after 120 minutes. It can be concluded that the strategy of NCS/CN composition improve the photocatalytic performance. When the content of NCS reached NCS-CN-3, the photocatalytic activity was the best.

The experimental data of photodegradation were fitted using a first-order kinetics model[14], which can be described by equation (2):

$$-\ln(C/C_0) = k_1 * t \quad (2)$$

where, k_1 (min^{-1}) and t are the first-order rate constant and time (min), respectively. Fig.4(b) shows the relation between $-\ln(C/C_0)$ and t. After linearly fitting of $-\ln(C/C_0)$ vs t, the values of k_1 are yielded, and showed in Table2. The coefficients of determination of the fitting (R^2) are also showed in Table2. All R^2 is greater than 0.91, which implies the photodegradation reactions are in good agreement with the first-order kinetics model.

The rate constant of NCS-CN-3 is 0.0061 min^{-1}, which is 3 and 3.4 times that of pure NCS and CN, respectively. The above results show that under the same experimental conditions, when the ratio of NCS in the composite is lower than NCS-CN-3, the efficiency of norfloxacin degradation can be improved with the increase of its content. When the ratio of NCS is greater than NCS-CN-3, the degradation efficiency is inversely proportional to the content of NCS. This result may be due to the excessive CNS covered on the surface of CN and obstructed the NORF absorption on CN.

Effect of pH on the removal of NORF by NCS-CN-3

Because pH value would not only affect the dispersibility of the catalyst and the type of surface charge in water, but also affect the characteristics of NORF antibiotic itself, pH would affect NORF photocatalytic degradation efficiency. Therefore, the influence of different pH values on the degradation reaction was investigated in this paper by conducting control group experiments. The results of the experiments were showed in Fig.5. When pH increased from 3 to 5, the final degradation rate of NORF increased significantly (from 11% to 31%). When pH was 7, the NORF degradation effect was the best, and the removal rate was 82%. When pH values were 9 and 11, the removal rates were 60% and 45%, respectively.

The reasons for the above results could be explained by the reaction mechanisms described by equations (3)-(6). When reaction system was acid(pH=3,5),the reaction step (equation (4)) was inhibited, and then the formation of radicals (•OH) were also restrained (equation (5));because of the lack of the radicals, NORF degradation(equation (6)) was inhibited. NORF is a weak carboxylic acid which pKa is 10.56. While in alkaline solution(pH=9,11), NORF became carboxylic anion which carried negative charger. According to the literature[15], in alkaline solution, the catalyst is negative charged, which would repel negatively charged NORF and slow down the photodegradation reaction speed.

$$NCS\text{-}CN + hv \rightarrow NCS(e^-)/CN(h^+) \quad (3)$$

$$H_2O \rightarrow H^+ + OH^- \quad (4)$$

$$CN(h^+) + OH^- \rightarrow CN + \bullet OH \quad (5)$$

$$NORF + \bullet OH \rightarrow Products \quad (6)$$

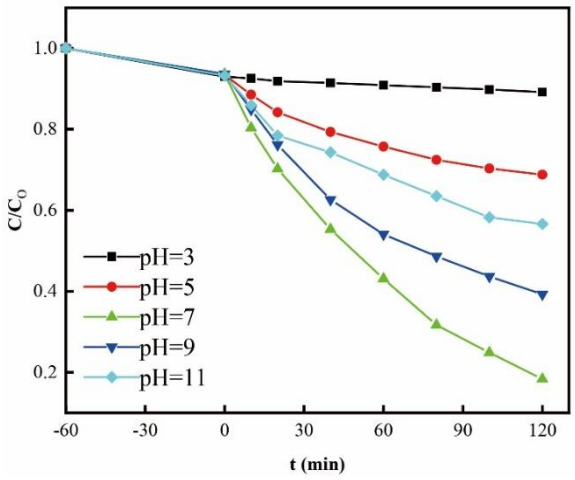

Fig. 5: Effect of different pH on the removal of NORF by NCS-CN-3. m/V=0.3g/L, $[NORF]_{initial}$=10mg/L, 298K.

Anion interference experiment

There are various anions, such as Cl^-, NO_3^-, and HCO_3^-, etc., in natural water environment. Therefore, the following control group experiments were conducted to explore the influence of different anions on NORF degradation efficiency. As can be seen from Fig. 6, when HCO_3^- was added to the photodegradation system, the degradation rate of NORF decreased significantly. When NO_3^- was added, the degradation rate was improved. When Cl^- was added, the degradation reaction was slightly inhibited. Therefore, in the presence of the above three anions, the degradability of NORF was $NO_3^- > Cl^- > HCO_3^-$.

The results above could be explained by the reaction mechanisms described by equations (7)-(10). It may be that NO_3^- anion produces active substances

in light, which forms a copromoting effect with the catalyst[16]. As shown in equation (8),(9), hydroxyl radical(•OH) and triplet atomic oxygen($O(^3p)$) could be formed when NO_3^- was activated by light in water, and prompted NORF photodegradation [16, 17].

When HCO_3^- was added in reactive system, the degradation of NORF was inhibited. It can be explained by equation (9) in which HCO_3^- reacted with •OH to form less active CO_3^-• [18].

$$H_2O + NO_3^- + hv \rightarrow \bullet OH + NO_2\bullet + OH^- \quad (7)$$

$$NO_3^- + hv \rightarrow NO_2^- + O(^3p) \quad (8)$$

$$HCO_3^- + \bullet OH \rightarrow H_2O + CO_3^-\bullet \quad (9)$$

$$Cl^- + \bullet OH \rightarrow ClOH^-\bullet \quad (10)$$

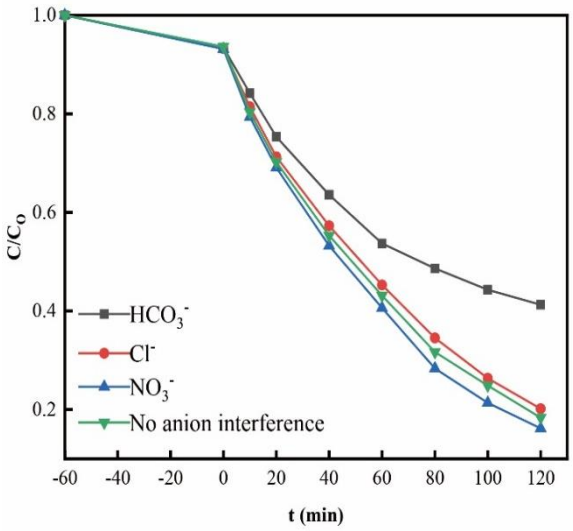

The degradation of NORF was slightly inhibited by Cl^- can be explained by equation(10) in which Cl^-reacted with •OH to form less active $ClOH^{\bullet -}$ [19].

Fig. 6: Effect of different anions on removal of NORF by NCS-CN-3. m/V=0.3g/L, initial pH=7, $[NORF]_{initial}$=10mg/L, 298K.

Reusability of composites

In order to verify the stability and reusability of the NCS-CN-3 composites, the material was continuously used 4 rounds as photodegradation catalyst under the same conditions. The results of four rounds were shown in Fig.7. Over four cycles, the degradation rate only declined from 0.805 to 0.745. These results confirmed that NCS-CN-3 had excellent stability and reusability. The photodegradation efficiency of cyclic experiments may be reduced because of light corrosion of a small amount of NCS in the composites.

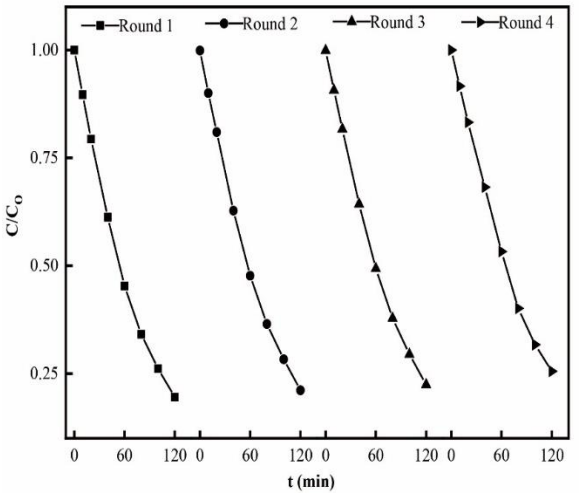

Fig. 7: Efficiency of removal of NORF by NCS-CN after 4 regeneration cycles. m/V=0.3g/L, initial pH=7, $[NORF]_{initial}$=10mg/L, 298K.

Free radical quenching experiments

In order to explore the photocatalytic reaction mechanism, it is necessary to determine the main active species in the photocatalytic process. Due to the difference in the ability of different catalysts to capture photogenerated electrons and holes, selective current peaks occur along the photogenerated electron transport path and affect the product distribution. Therefore, ethylenediamine (EDTA), isopropyl alcohol (IPA) and benzoquinone (BQ) were added to the reaction system as h^+, •OH and $\bullet O_2^-$ scavengers, so as to distinguish which class of active substances played a role. As shown in Fig.8, after EDTA and BQ were added, the degradation rate of NORF decreased significantly, reaching 58% and 25% respectively in 120 min. However, there was little change in the degradation curve when IPA was added, indicating that •OH was not the active substances and h^+, O_2^- were the active substances that catalyzed the degradation reaction, among which $\bullet O_2^-$ played a major role.

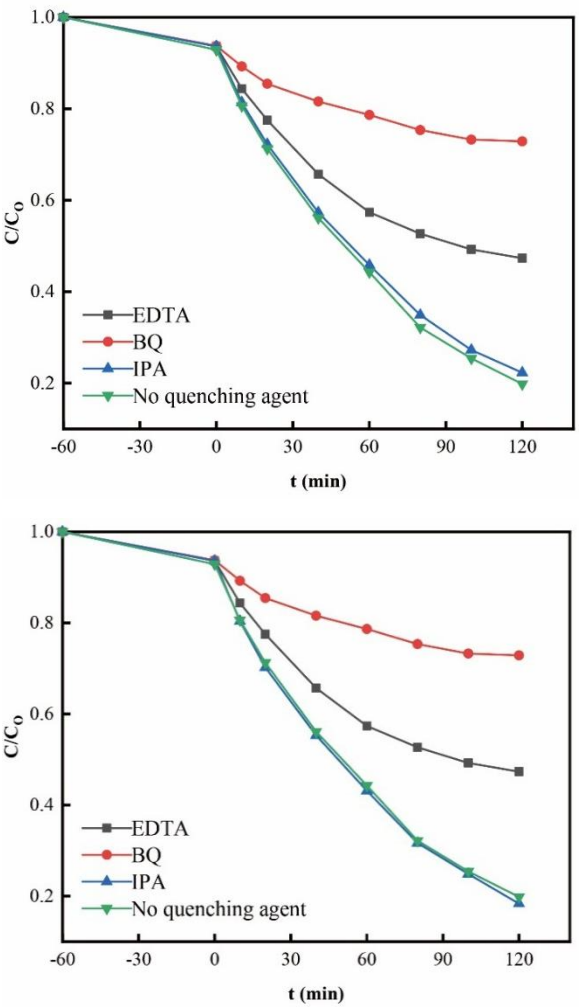

Fig. 8: Effects of different free radical quenching agents on NORF degradation efficiency. m/V=0.3g/L, initial pH=7, $[NORF]_{initial}$=10mg/L, 298K.

Photocatalytic reaction mechanism

According to the literature [20], the photodegradation mechanism of norfloxacin (NORF) by NCS/NC in water is illustrated in Figure 9. In the NCS/CN composite material, the Z-scheme charge transfer mechanism [21] plays a pivotal role, where CN absorbs visible light and becomes excited, generating electron-hole pairs. In this system, NCS acts as the electron acceptor, and its nanostructure enhances the establishment of an internal electric field. This strong driving force leads to the rapid separation of the electron-hole pairs within the NCS/CN heterogeneous structure, allowing a substantial number of photogenerated electrons to effectively migrate to the conduction band (CB) of NCS, thereby facilitating charge transfer. During this process, a dynamic equilibrium is established between the photogenerated holes and the electrons captured by NCS, promoting a more efficient reaction through this Type II transfer mechanism. Studies have shown that the conduction band potential of NCS is more negative than the $O_2/•O_2^-$ (−0.33 eV) redox potential; consequently, dissolved oxygen can be reduced to superoxide anions ($•O_2^-$) by the photogenerated electrons, effectively contributing to the decomposition of NORF molecules. Simultaneously, the accumulating photogenerated holes in the valence band (VB) of CN serve as key active species promoting the degradation of NORF. However, the valence band potential of CN (+1.22 eV) is lower than the redox potential of $•OH/OH^-$ (+2.27 eV) [23]. Therefore, the holes (h+) in the valence band of CN lack sufficient energy to oxidize OH^- to form •OH, rendering the role of •OH in the degradation of NORF negligible, which aligns with the experimental results presented in Figure 8.

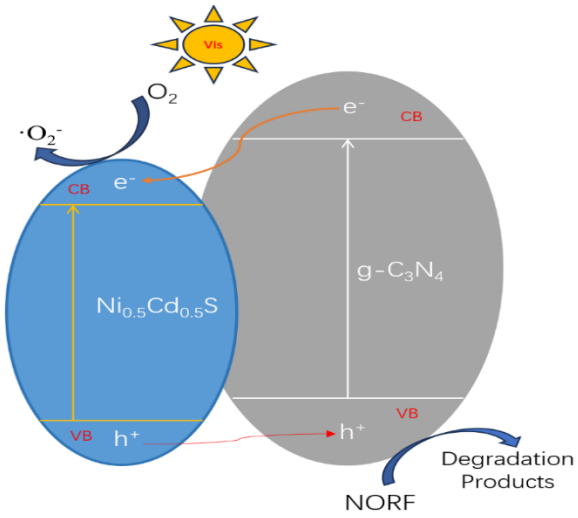

Fig. 9: Diagram of photocatalytic reaction mechanism.

Conclusion

NCS nanoparticles were combined with CN nanosheets by hydrothermal method. The composition, crystallinity, morphology of NCS/CN composites were characterized by X-ray diffractometer, SEM, EDS. The results show that NCS was uniformly distributed on nanosheet CN. NORF photodegradation experiments proved that NCS-CN-3 was the most

effective catalyst. The best photocatalysis reaction pH was neutral. The interfering anions experiments results showed that NORF degradability were promoted by NO_3^-, obviously inhibited by HCO^- and slightly inhibited by Cl^-.The experiments of free radicals quenching showed that main active substances in NORF degradation were O_2^- and h^+.

Acknowledgements

This work was supported by the PhD research startup foundation of Anhui Jianzhu University (2020QDZ33), Anhui Province Advanced building materials International Joint Research Center director fund (JZCL2411ZR), Natural Science Research Key Project from Education Department of Anhui Province (2023AH050190, KJ2021A0626), Equipment & Demonstration Project for Chemical Remediation of Organic Contaminated Soil & Groundwater in Low Permeability Strata by Insitu Injection Method (HYB20230209). the Natural Science Foundation of Anhui Province (2308085QB66,2008085MB57)

References

1. J. L. Liu and M. H. Wong, Pharmaceuticals and personal care products (PPCPs): A review on environmental contamination in China, *Environment International*, **59**, 208 (2013).
2. C. Su, Y. Cui, D. Liu, H. Zhang, Y. Baninla, Endocrine disrupting compounds, pharmaceuticals and personal care products in the aquatic environment of China: Which chemicals are the prioritized ones?, *Sci. Total Environ*., **720** 137652 (2020).
3. S. Zeng, J. Sun, X. Lü, Z. Peng, B. Dong, X. Dai, B. J. Ni, Impacts of norfloxacin on sewage sludge anaerobic digestion: Bioenergy generation and potential environmental risks, *Results in Engineering*, **20**, 101392 (2023).
4. X. Fang, S. Wu, Y. Wu, W. Yang, Y. Li, J. he, P. Hong, M. Nie, C. Xie, Z. Wu, Z. Kaisheng, L. Kong, J. Liu, High-efficiency adsorption of norfloxacin using octahedral UIO-66-NH2 nanomaterials: Dynamics, thermodynamics, and mechanisms, *Applied Surface Science,* **518** 146226 (2020).
5. S. P. Preethi, G. Shanmugavel, Y. K. Kumar, Recent progress in mineralization of emerging contaminants by advanced oxidation process: A review, *Environmental Pollution*, **341** 122842 (2024).
6. P. Luo, Y. Zhang, Z. Peng, Q. He, W. Zhao, W. Zhang, D. Yin, Y. Zhang, J. Tang, Photocatalytic degradation of perfluorooctanoic acid (PFOA) from water: A mini review, *Environmental Pollution*, **343**, 123212 (2024).
7. C. Bozkaplan, A. Tombak, M.F. Genişel, Y.S. Ocak, K. Akkilic, The influence of substrate temperature on RF sputtered CdS thin films and CdS/p-Si heterojunctions, *Materials Science in Semiconductor Processing,* **58**, 34 (2017).
8. Y. K. Ramgolam and K. M. S. Soyjaudah, Modelling the impact of spectral irradiance and average photon energy on photocurrent of solar modules, *Solar Energy*, **173**, 1058 (2018).
9. M. Norton, A.M.G. Amillo, R. Galleano, Comparison of solar spectral irradiance measurements using the average photon energy parameter, *Solar Energy*, **120**, 337 (2015).
10. N. H. Patel, M.P. Deshpande, S.H. Chaki, H.R. Keharia, Optical and Thermal Studies of Pristine and Ni Doped CdS Nanoparticles with Antibacterial Applications, *Materials Focus*, **6** 398 (2017).
11. G. Mamba, A.K. Mishra, Graphitic carbon nitride (g-C3N4) nanocomposites: A new and exciting generation of visible light driven photocatalysts for environmental pollution remediation, *Applied Catalysis B: Environmental,* **198**, 347 (2016).
12. H. Xu, L. Wu, L. Jin, K. Wu, Combination Mechanism and Enhanced Visible-Light Photocatalytic Activity and Stability of CdS/g-C3N4 Heterojunctions, *Journal of Materials Science & Technology*, **33**, 30 (2017).
13. P. R. Jubu, F. K. Yam, V. M. Igba, K. P. Beh, Tauc-plot scale and extrapolation effect on bandgap estimation from UV–vis–NIR data – A case study of β-Ga2O3, *Journal of Solid State Chemistry*, **290**, 121576 (2020).
14. Z. Wu, Q. Chen, S. Wu, Photocatalytic degradation of norfloxacin antibiotics on ZnxCd(1-x)S/g-C3N4 composites in water, *Environmental Science and Pollution Research*, (2024).
15. Z. Qiang, C. Adams, Potentiometric determination of acid dissociation constants (pKa) for human and veterinary antibiotics, *Water Research*, **38**, 2874 (2004) .
16. O.C. Zafiriou, M.B. True, Nitrate photolysis in seawater by sunlight, *Marine Chemistry*, **8**, 33 (1979).
17. C. Yu, H. Wang, X. Liu, X. Quan, S. Chen, J. Zhang, P. Zhang, Photodegradation of 2,4-D induced by NO2− in aqueous solutions: The role of NO_2, *Journal of Environmental Sciences*, **26,** 1383 (2014).

18. K. H. Choo, D.-I. Chang, K.-W. Park, M.-H. Kim, Use of an integrated photocatalysis/hollow fiber microfiltration system for the removal of trichloroethylene in water, *Journal of Hazardous Materials*, **152**, 183 (2008).
19. Z. Zhao, J. Zhao, C. Yang, Efficient removal of ciprofloxacin by peroxymonosulfate/Mn3O4-MnO2 catalytic oxidation system, *Chemical Engineering Journal*, **327**, 481 (2017).
20. J. Fu, B. Chang, Y. Tian, F. Xi, X. Dong, Novel C3N4–CdS composite photocatalysts with organic–inorganic heterojunctions: in situ synthesis, exceptional activity, high stability and photocatalytic mechanism, *Journal of Materials Chemistry A*, **1**, 3083 (2013).
21. H. S. Wenhua Xue, Xiaoyun Hu, Xue Bai, Jun Fan, Enzhou Liu, UV-VIS-NIR-induced extraordinary H2 evolution over W18O49/Cd0.5Zn0.5S: Surface plasmon effect coupled with S-scheme charge transfer *Chinese Journal of Catalysis*, **43**, 234 (2022).
22. G. Wang, Z. Jin, Rationally Designed Functional Ni2P Nanoparticles as Co–Catalyst Modified CdS@g-C3N4 Heterojunction for Efficient Photocatalytic Hydrogen Evolution, *ChemistrySelect*, **4**, 3602 (2019).
23. Y. Tian, B. Chang, Z. Yang, B. Zhou, F. Xi, X. Dong, Graphitic carbon nitride–BiVO4 heterojunctions: simple hydrothermal synthesis and high photocatalytic performances, *RSC Advances*, **4**, 4187 (2014).